Supplementary information on the article:

Coherent soliton states hidden in phase-space and stabilized by gravitational incoherent structures

Josselin Garnier[1], Kilian Baudin[2], Adrien Fusaro[2,3], Antonio Picozzi[2]

[1] *CMAP, CNRS, Ecole Polytechnique, Institut Polytechnique de Paris, 91128 Palaiseau Cedex, France*

[2] *Laboratoire Interdisciplinaire Carnot de Bourgogne, CNRS, Université Bourgogne Franche-Comté, 21078 Dijon, France and*

[3] *CEA, DAM, DIF, F-91297 Arpajon Cedex, France*

I. NUMERICAL TECHNIQUES

A. SPE in a finite box for simulations

The numerical simulations are carried out on a system set in a bounded domain with prescribed boundary conditions:

$$i\partial_t \psi + \frac{\alpha}{2}\Delta_{\boldsymbol{x}}\psi - V_L\psi = 0, \tag{S1}$$

$$V_L = -\gamma U_{D,L} * |\psi|^2, \tag{S2}$$

where $\boldsymbol{x} \in [-L/2, L/2]^D$ with periodic boundary conditions. Here $U_{D,L}(\boldsymbol{x})$ is the periodic function equal to $U_D(\boldsymbol{x}) - c_{D,L}$ in $[-L/2, L/2]^D$ and $c_{D,L} = L^{-D}\int_{[-L/2,L/2]^D} U_D(\boldsymbol{x})d\boldsymbol{x}$ so that $U_{D,L}$ has mean zero. Eq. (S2) is equivalent to $V_L = -\gamma U_D * (|\psi|^2 - \bar{\rho}_L)$, with $\bar{\rho}_L = L^{-D}\int_{[-L/2,L/2]^D} |\psi(\boldsymbol{x})|^2 d\boldsymbol{x}$, and V_L in the simulations has zero mean. The potential V_L is numerically computed by Fourier transform [1]. Note that the formulation Eqs.(1-2) in the open medium (used for the theoretical analysis) and (S1-S2) in the periodic medium (used for the numerical analysis) have an apparent departure in the definitions of the potential U which differ by a constant. However, the substraction of the constant $c_{D,L}$ to U_D can be removed by multiplying ψ by $\exp(-i\gamma c_{D,L}Mt)$, with $M = \int_{[-L/2,L/2]^D} |\psi(\boldsymbol{x})|^2 d\boldsymbol{x} = L^D\bar{\rho}_L$.

Jeans length: The growth-rate of the gravitational instability in $\sigma_{\rm inst} = \sqrt{\alpha\eta_D\gamma\bar{\rho} - \alpha^2k^4/4}$, so that modes with $k \geq k_J = 2\pi/\Lambda_J$ with $\Lambda_J = \sqrt{2}\pi(\alpha/(\gamma\eta_D\bar{\rho}))^{1/4}$ are stable. $\Lambda = (\alpha/(2\gamma\bar{\rho}))^{1/4} \simeq \Lambda_J$ is the normalizing length scale used in the simulations in Figs. 1-3. We solved numerically the dimensionless SPE: $i\partial_{\tilde{t}}\tilde{\psi} = -\nabla^2_{\tilde{\boldsymbol{x}}}\tilde{\psi} - \tilde{\psi}\tilde{U}_{D,L} * |\tilde{\psi}|^2$, with $\tilde{\boldsymbol{x}} = \boldsymbol{x}/\Lambda$, $\tilde{t} = t/\tau$, $\tilde{\psi} = \psi/\sqrt{\bar{\rho}}$, $\tau = 2\Lambda^2/\alpha$ and $\tilde{L} = L/\Lambda = 135$ in Figs. 1-3.

De Broglie wavelength: It is defined by $\lambda_{\rm dB} = h/(mv)$, where v is the 'hydrodynamic' velocity defined from the gradient of the phase φ of $\psi = \sqrt{\rho}\exp(i\varphi)$. With our notations $\boldsymbol{v} = \alpha\nabla\varphi$, so that $\lambda_{\rm dB} = 2\pi/|\nabla\phi| \sim 2\pi\lambda_c$ where λ_c is the correlation radius of ψ.

B. Wigner and Husimi transforms, and the optical spectrogram

The empirical Wigner transform

$$W(\boldsymbol{k}, \boldsymbol{x}, t) = \int \psi(\boldsymbol{x} + \boldsymbol{y}/2, t)\psi^*(\boldsymbol{x} - \boldsymbol{y}/2, t)\exp(-i\boldsymbol{k}\cdot\boldsymbol{y})\, d\boldsymbol{y}, \tag{S3}$$

is not statistically stable (its standard deviation is larger than its statistical average). It is necessary to smooth it with respect to $\boldsymbol{k}$ and $\boldsymbol{x}$ to get a statistically stable quantity. We consider the smoothed Wigner transform or Husimi function

$$W_\sigma(\boldsymbol{k}, \boldsymbol{x}, t) = \frac{1}{\pi^2}\iint W(\boldsymbol{k}', \boldsymbol{x}', t)\exp\Big(-\frac{|\boldsymbol{x} - \boldsymbol{x}'|^2}{\sigma^2} - \sigma^2|\boldsymbol{k} - \boldsymbol{k}'|^2\Big)d\boldsymbol{k}'d\boldsymbol{x}', \tag{S4}$$

which can also be written as

$$W_\sigma(\boldsymbol{k}, \boldsymbol{x}, t) = \frac{1}{\pi\sigma^2}\Big|\int \psi(\boldsymbol{y})\exp\Big(-\frac{|\boldsymbol{x} - \boldsymbol{y}|^2}{2\sigma^2}\Big)\exp(-i\boldsymbol{k}\cdot\boldsymbol{y})d\boldsymbol{y}\Big|^2. \tag{S5}$$

This quantity is statistically stable for all $\sigma > 0$. When the field is fully incoherent the standard deviation of W_σ is equal to its average, more exactly, W_σ follows an exponential distribution because it is the square modulus a circular complex Gaussian random variable by (S5). A small (resp. large) σ means that the smoothing is smaller (resp. larger) in $\boldsymbol{x}$ than in $\boldsymbol{k}$ by (S4). A good trade-off (with equal smoothing in $\boldsymbol{x}$ and $\boldsymbol{k}$) is achieved by choosing $\sigma \simeq \sqrt{\Delta x/\Delta k}$ when the radius of n is Δk in $\boldsymbol{k}$ and Δx in $\boldsymbol{x}$.

Relation with the optical spectrogram: The measurement of the Husimi transform is known in optics as the 'spectrogram'. It is measured by performing a windowed Fourier transform by passing the beam through a small aperture (Gaussian in (S5)), whose spatial position is scanned along the optical beam [2].

II. DERIVATION OF THE EFFECTIVE SPE, EQ.(6)

A. System of coupled SPE and WT-VPE, Eqs.(4-5)

The hidden solitons are characterized by a non-vanishing average $\langle \psi \rangle \neq 0$, so that we decompose the field into a coherent component $A(\boldsymbol{x}, t)$ and an incoherent component $\phi(\boldsymbol{x}, t)$ of zero mean ($A = \langle A \rangle \neq 0, \langle \phi \rangle = 0$):

$$\psi(\boldsymbol{x}, t) = A(\boldsymbol{x}, t) + \phi(\boldsymbol{x}, t). \tag{S6}$$

Following the usual procedure [3], we define the spectrum of the IS as $n(\boldsymbol{k}, \boldsymbol{x}, t) = \int C(\boldsymbol{x}, \boldsymbol{y}, t) \exp(-i\boldsymbol{k} \cdot \boldsymbol{y})\, d\boldsymbol{y}$, where the correlation function $C(\boldsymbol{x}, \boldsymbol{y}, t) = \langle \phi(\boldsymbol{x} + \boldsymbol{y}/2, t)\phi^*(\boldsymbol{x} - \boldsymbol{y}/2, t)\rangle$, is defined from an average over the realizations $\langle \cdot \rangle$. Starting from the SPE (1-2), we obtain Eqs.(4-5) (main text):

$$i\partial_t A = -\frac{\alpha}{2}\nabla^2 A + AV, \tag{S7}$$

$$\partial_t n(\boldsymbol{k}, \boldsymbol{x}) + \alpha \boldsymbol{k} \cdot \partial_{\boldsymbol{x}} n(\boldsymbol{k}, \boldsymbol{x}) - \partial_{\boldsymbol{x}} V \cdot \partial_{\boldsymbol{k}} n(\boldsymbol{k}, \boldsymbol{x}) = 0, \tag{S8}$$

which are coupled to each other by the *averaged* long-range gravitational potential

$$V(\boldsymbol{x}, t) = -\gamma \int U_D(\boldsymbol{x} - \boldsymbol{y})\big(|A|^2(\boldsymbol{y}, t) + \rho_{IS}(\boldsymbol{y}, t)\big) d\boldsymbol{y}, \tag{S9}$$

$$\rho_{IS}(\boldsymbol{x}, t) = \big\langle |\phi(\boldsymbol{x}, t)|^2 \big\rangle = \frac{1}{(2\pi)^D} \int n(\boldsymbol{k}, \boldsymbol{x}, t) d\boldsymbol{k}. \tag{S10}$$

Validity of the WT-VPE: The WT-VPE (S8) is valid beyond the weakly nonlinear regime [3]. Thanks to the long-range nature of the interaction, the system exhibits a self-averaging property of the nonlinear response, $\int U_D(\boldsymbol{x} - \boldsymbol{y})|\phi(\boldsymbol{y})|^2 d\boldsymbol{y} \simeq \int U_D(\boldsymbol{x} - \boldsymbol{y}) \big\langle |\phi(\boldsymbol{y})|^2 \big\rangle\, d\boldsymbol{y}$. Substitution of this property into the SPE leads to an automatic closure of the hierarchy of the moment equations. Using statistical arguments similar to those in Ref.[4], one can show that, owing to a highly nonlocal response, the statistics of the incoherent wave turns out to be Gaussian.

Distinction with the Boltzmann VPE: It is important to distinguish the WT-VPE (S8) from the collisionless Boltzmann VPE [5, 6]: At variance with the VPE describing a spiky distribution, the WT-VPE describes the smooth evolution of the second-order moment $n(\boldsymbol{k}, \boldsymbol{x})$ defined from the *average* over the realizations $\langle \cdot \rangle$.

B. Multi-scale expansion theory to derive the effective SPE [Eq.(6)]

The partially coherent field ψ is of the form (S6). It is composed of a coherent soliton $A(\boldsymbol{x}, t)$ and an IS characterized by its spectrum $n(\boldsymbol{k}, \boldsymbol{x}, t)$. They satisfy the coupled equations (S7-S8) with the long-range potential (S9). The average density $\rho_{IS}(\boldsymbol{x}, t)$ can be expressed in terms of the spectrum n as (S10). We show that the scaling regime $A(\boldsymbol{x}, t) = A^{(0)}(\boldsymbol{x}, t)$, $n(\boldsymbol{k}, \boldsymbol{x}, t) = \varepsilon^D n^{(0)}(\varepsilon \boldsymbol{k}, \varepsilon \boldsymbol{x}, t)$ described in the main text is the correct one to describe a hidden soliton stabilized by the IS. We look for solutions of the form

$$n(\boldsymbol{k}, \boldsymbol{x}, t) = \varepsilon^p n^{(0)}(\varepsilon^q \boldsymbol{k}, \varepsilon^r \boldsymbol{x}, \varepsilon^s t), \qquad A(\boldsymbol{x}, t) = \varepsilon^v A^{(0)}(\varepsilon^w \boldsymbol{x}, \varepsilon^z t), \tag{S11}$$

where $\varepsilon \ll 1$ is a small dimensionless quantity that characterizes the scaling ratios between the different characteristic length scales and amplitudes of the coherent and incoherent fields. With (S11) we also have $\rho_{IS}(\boldsymbol{x}, t) = \varepsilon^{p-Dq} \rho_{IS}^{(0)}(\varepsilon^r \boldsymbol{x}, \varepsilon^s t)$ with $\rho_{IS}^{(0)}(\boldsymbol{X}, T) = \int n^{(0)}(\boldsymbol{K}, \boldsymbol{X}, T) d\boldsymbol{K}$. We look for solutions with $r > w$, i.e., we look for a soliton whose radius is small compared to the typical radius of the IS.

I) We first look at the equations at the scale of the soliton. If $\boldsymbol{x} = \varepsilon^{-w}\boldsymbol{X}$, $t = \varepsilon^{-z}T$, then

$$(U_D * |A|^2)A(\boldsymbol{x}, t) = \varepsilon^{3v-2w}(U_D * |A^{(0)}|^2)A^{(0)}(\boldsymbol{X}, T),$$
$$\Delta_{\boldsymbol{x}} A(\boldsymbol{x}, t) = \varepsilon^{v+2w}\Delta_{\boldsymbol{X}} A^{(0)}(\boldsymbol{X}, T),$$
$$\partial_t A(\boldsymbol{x}, t) = \varepsilon^{v+z}\partial_T A^{(0)}(\boldsymbol{X}, T).$$

We also have

$$(U_D * \rho_{IS})(\boldsymbol{x}, t) = \varepsilon^{p-Dq-2r} \int U_D(\boldsymbol{Y}) \rho_{IS}^{(0)}(\boldsymbol{Y} + \varepsilon^{r-w}\boldsymbol{X}, T) d\boldsymbol{Y}.$$

Since $r > w$ we can expand

$$\int U_D(\boldsymbol{Y})\rho_{IS}^{(0)}(\boldsymbol{Y}+\varepsilon^{r-w}\boldsymbol{X},T)d\boldsymbol{Y} = \int U_D(\boldsymbol{Y})\rho_{IS}^{(0)}(\boldsymbol{Y},\varepsilon^{z-s}T)d\boldsymbol{Y} + \varepsilon^{r-w}\boldsymbol{X}\cdot\Big[\int U_D(\boldsymbol{Y})\nabla_{\boldsymbol{Y}}\rho_{IS}^{(0)}(\boldsymbol{Y},\varepsilon^{z-s}T)d\boldsymbol{Y}\Big] + \frac{1}{2}\varepsilon^{2r-2w}\boldsymbol{X}\cdot\Big[\int U_D(\boldsymbol{Y})\nabla_{\boldsymbol{Y}}\otimes\nabla_{\boldsymbol{Y}}\rho_{IS}^{(0)}(\boldsymbol{Y},\varepsilon^{z-s}T)d\boldsymbol{Y}\Big]\boldsymbol{X} + o(\varepsilon^{2r-2w}).$$

The first term is a constant in $\boldsymbol{X}$ that depends only on T. If $\rho_{IS}^{(0)}$ is spherically symmetric then the second term is zero and the third term takes the form

$$\int U_D(\boldsymbol{Y})\rho_{IS}^{(0)}(\boldsymbol{Y}+\varepsilon^{r-w}\boldsymbol{X},T)d\boldsymbol{Y} = const_\varepsilon + \frac{1}{2D}\varepsilon^{2r-2w}\Big[\int U_D(\boldsymbol{Y})\Delta_{\boldsymbol{Y}}\rho_{IS}^{(0)}(\boldsymbol{Y},\varepsilon^{z-s}T)d\boldsymbol{Y}\Big]|\boldsymbol{X}|^2 + o(\varepsilon^{2r-2w}).$$

After integrating by parts and using $\Delta_{\boldsymbol{Y}}U_D(\boldsymbol{Y}) = -\eta_D\delta(\boldsymbol{Y})$, we get

$$\int U_D(\boldsymbol{Y})\rho_{IS}^{(0)}(\boldsymbol{Y}+\varepsilon^{r-w}\boldsymbol{X},T)d\boldsymbol{Y} = const_\varepsilon - q_D\varepsilon^{2r-2w}\rho_{IS}^{(0)}(\boldsymbol{0},\varepsilon^{z-s}T)|\boldsymbol{X}|^2 + o(\varepsilon^{2r-2w}), \tag{S12}$$

where $q_D = \eta_D/(2D)$, and therefore

$$(U_D * \rho_{IS})A(\boldsymbol{x},t) = const_\varepsilon A^{(0)}(\boldsymbol{X},T) - q_D\varepsilon^{v+p-Dq-2w}\rho_{IS}^{(0)}(\boldsymbol{0},\varepsilon^{z-s}T)|\boldsymbol{X}|^2A^{(0)}(\boldsymbol{X},T) + o(\varepsilon^{v+p-Dq-2w}).$$

The term $const_\varepsilon A^{(0)}$ plays no role because it only gives a time-dependent phase term in (S7). We require the ε-terms to be balanced in (S7) because we look for a solution in the form of a soliton stabilized by the IS. The terms are balanced if $3v-2w = v+p-Dq-2w = v+2w = v+z$, that is to say, if

$$(p-Dq)/2 = 2w = v = z. \tag{S13}$$

II) We next look at the equations at the scale of the IS. If $\boldsymbol{x} = \varepsilon^{-r}\boldsymbol{X}$, $\boldsymbol{k} = \varepsilon^{-q}\boldsymbol{K}$, $t = \varepsilon^{-s}T$, then (using $r > w$)

$$(U_D * |A|^2)(\boldsymbol{x},t) = \varepsilon^{2v-r(2-D)-wD}U_D(\boldsymbol{X})\int |A^{(0)}(\boldsymbol{X}',\varepsilon^{s-z}T)|^2d\boldsymbol{X}' + o(\varepsilon^{2v-r(2-D)-wD}),$$
$$(U_D * \rho_{IS})(\boldsymbol{x},t) = \varepsilon^{p-Dq-2r}U_D * \rho_{IS}^{(0)}(\boldsymbol{X},T).$$

Thus

$$\partial_{\boldsymbol{x}}V(\boldsymbol{x},t)\cdot\partial_{\boldsymbol{k}}n(\boldsymbol{k},\boldsymbol{x},t) = \varepsilon^{2p-(D-1)q-r}\partial_{\boldsymbol{X}}\big(U_D * \rho_{IS}^{(0)}\big)(\boldsymbol{X},T)\cdot\partial_{\boldsymbol{K}}n^{(0)}(\boldsymbol{K},\boldsymbol{X},T) + \varepsilon^{p+q+2v-r(1-D)-wD}\partial_{\boldsymbol{X}}\Big(U_D(\boldsymbol{X})\int |A^{(0)}(\boldsymbol{X}',\varepsilon^{s-z}T)|^2d\boldsymbol{X}'\Big)\cdot\partial_{\boldsymbol{K}}n^{(0)}(\boldsymbol{K},\boldsymbol{X},T),$$
$$\boldsymbol{k}\cdot\partial_{\boldsymbol{x}}n(\boldsymbol{k},\boldsymbol{x},t) = \varepsilon^{p-q+r}\boldsymbol{K}\cdot\partial_{\boldsymbol{X}}n^{(0)}(\boldsymbol{K},\boldsymbol{X},t),$$
$$\partial_t n(\boldsymbol{k},\boldsymbol{x},t) = \varepsilon^{p+s}\partial_T n^{(0)}(\boldsymbol{K},\boldsymbol{X},t).$$

We look for balanced terms in (S8) amongst the components coming the IS, because we do not look for a solution in which the IS would be affected by the soliton. The terms are balanced provided $2p-(D-1)q-r = p-q+r = p+s$, namely

$$r = (p-(D-2)q)/2 \quad \text{and} \quad s = (p-Dq)/2. \tag{S14}$$

III) Conclusion: Without loss of generality, we can choose the reference length scale to be the radius of the soliton, that is to say, we can choose $w = 0$. Then we get balanced terms in equations in (S7) and (S8) provided conditions (S13) and (S14) are satisfied, which means

$$w = v = s = z = 0, \quad q = r > 0, \quad p = Dq. \tag{S15}$$

In this case we can check that $p+q+2v-r(1-D)-wD = 2Dq > (2D-1)q = 2p-r$, which shows that the soliton has no influence on the IS:

$$\partial_{\boldsymbol{x}}V\cdot\partial_{\boldsymbol{k}}n(\boldsymbol{k},\boldsymbol{x},t) = \varepsilon^{Dq}\partial_{\boldsymbol{X}}\big(U_D * \rho_{IS}^{(0)}\big)(\boldsymbol{X},T)\cdot\partial_{\boldsymbol{K}}n^{(0)}(\boldsymbol{K},\boldsymbol{X},T) + o(\varepsilon^{Dq}).$$

We can take without loss of generality $q = r = 1$ and $p = D$, because the small dimensionless parameter ε is arbitrary. We then obtain $A(\boldsymbol{x},t) = A^{(0)}(\boldsymbol{x},t)$, $n(\boldsymbol{k},\boldsymbol{x},t) = \varepsilon^D n^{(0)}(\varepsilon\boldsymbol{k},\varepsilon\boldsymbol{x},t)$, the SPE (S7) takes the form

$$i\partial_t A^{(0)}(\boldsymbol{x},t) = -\frac{\alpha}{2}\nabla^2 A^{(0)}(\boldsymbol{x},t) - \gamma(U_D * |A^{(0)}|^2)A^{(0)}(\boldsymbol{x}) + \gamma q_D\rho_{IS}^{(0)}(\boldsymbol{0},t)|\boldsymbol{x}|^2A^{(0)}(\boldsymbol{x}), \tag{S16}$$

that is to say the effective SPE Eq.(6) (main text), and the WT-VPE (S8) takes the form (with $\boldsymbol{X}=\varepsilon \boldsymbol{x}$ and $\boldsymbol{K}=\varepsilon \boldsymbol{k}$)

$$\partial_t n^{(0)}(\boldsymbol{K},\boldsymbol{X},t)+\alpha \boldsymbol{K}\cdot\partial_{\boldsymbol{X}} n^{(0)}(\boldsymbol{K},\boldsymbol{X},t)+\gamma\partial_{\boldsymbol{X}}(U_D*\rho_{IS}^{(0)})(\boldsymbol{X},t)\cdot\partial_{\boldsymbol{K}} n^{(0)}(\boldsymbol{K},\boldsymbol{X},t)=0. \tag{S17}$$

This rescaled form of the WT-VPE does not depend on the coherent component, i.e., on the soliton dynamics.

Justification of the scale separations of the new regime Eq.(3): The scaling $A(\boldsymbol{x},t)=A^{(0)}(\boldsymbol{x},t)$, $n(\boldsymbol{k},\boldsymbol{x},t)=\varepsilon^D n^{(0)}(\varepsilon\boldsymbol{k},\varepsilon\boldsymbol{x},t)$ also implies all of the separation of spatial scales involved in the new regime reported in our work, namely $\tilde{\xi}=\xi/\Lambda=\varepsilon$, $\lambda_c/\Lambda=O(\varepsilon)$, $\ell/\Lambda=O(\varepsilon^{-1})$, $R_S/\Lambda=O(1)$, $|A|^2\sim O(1)$, $n\sim\varepsilon^D$ and $\rho_{IS}\sim 1$. This gives Eq.(3):

$$\lambda_c\sim\xi\ll R_S\sim\Lambda\ll\ell \qquad\text{and}\qquad \rho_S\sim\bar{\rho}_{IS}.$$

III. BINARY SOLITON: 3D DYNAMICS AND DERIVATION OF EQS.(7-10)

We study the dynamics of the binary soliton system for $D=1$ and $D=3$. The Lagrangian of the effective SPE (S16) is

$$\mathcal{L}=\int \frac{i}{2}\big(A\partial_t A^*-\partial_t A A^*\big)+\frac{\alpha}{2}|\nabla A|^2+\frac{1}{2}V_S(\boldsymbol{x})|A|^2+q_D\gamma\rho_0|\boldsymbol{x}|^2|A|^2 d\boldsymbol{x}, \tag{S18}$$

where $V_S(\boldsymbol{x},t)=-\gamma\int U_D(\boldsymbol{x}-\boldsymbol{y})|A|^2(\boldsymbol{y},t)d\boldsymbol{y}$, with $q_1=1$, $q_3=2\pi/3$, $U_1(x)=-|x|$, $U_3(\boldsymbol{x})=1/|\boldsymbol{x}|$, and $\rho_0(t)=\rho_{IS}(\boldsymbol{x}=\boldsymbol{0},t)$ is the average density of the incoherent structure at the center. We consider the Gaussian ansatz for a two-component soliton:

$$A(\boldsymbol{x},t)\ =\ \sum_{j=1}^{2}a_j(t)\exp\Big(-\frac{|\boldsymbol{x}-\boldsymbol{x}_{o,j}(t)|^2}{2R_j^2(t)}+ib_j(t)|\boldsymbol{x}-\boldsymbol{x}_{o,j}(t)|^2+i\boldsymbol{k}_{o,j}(t)\cdot(\boldsymbol{x}-\boldsymbol{x}_{o,j}(t))+i\nu_j(t)\Big).$$

The effective Lagrangian depends on $a_j(t)$, $R_j(t)$, $b_j(t)$, $\nu_j(t)$, $\boldsymbol{x}_{o,j}(t)$ and $\boldsymbol{k}_{o,j}(t)$ and their time derivatives. It can be split into three parts. The first two parts depend on each of the components of the coherent structure, the third part represents the interaction between the two components $\mathcal{L}=\mathcal{L}_1+\mathcal{L}_2+\mathcal{L}_{12}$:

$$\begin{aligned}\mathcal{L}_j&=M_{S,j}\Big(\partial_t\nu_j+D\partial_t b_j\frac{R_j^2}{2}-\boldsymbol{k}_{o,j}\cdot\partial_t\boldsymbol{x}_{o,j}\Big)+\frac{\alpha M_{S,j}}{4}\big(\frac{D}{R_j^2}+4Db_j^2R_j^2+2|\boldsymbol{k}_{o,j}|^2\big)\\&\quad-\frac{\gamma}{\sqrt{2\pi}}M_{S,j}^2R_j^{2-D}+\gamma\rho_0 q_D M_{S,j}\big(\frac{D}{2}R_j^2+|\boldsymbol{x}_{o,j}|^2\big),\\ \mathcal{L}_{12}&=-\gamma M_{S,1}M_{S,2}|\boldsymbol{x}_{o,1}-\boldsymbol{x}_{o,2}|^{2-D},\end{aligned}$$

where $M_{S,j}=a_j^2\pi^{D/2}R_j^D$ is the mass of the j-th component of the coherent structure and we have assumed that $|\boldsymbol{x}_{o,1}-\boldsymbol{x}_{o,2}|\gg R_1,R_2$ in order to simplify $\mathcal{L}_{12}$. The evolution equations for the parameters of the ansatz are then derived from the effective Lagrangian by using the corresponding Euler-Lagrange equations $\delta\int\mathcal{L}dt=0$ [7]. We obtain the closed-form ordinary differential equation for the width R_j of the j-th component of the coherent structure:

$$\partial_t^2 R_j=\frac{\alpha^2}{R_j^3}-\sqrt{\frac{2}{\pi}}\frac{\alpha\gamma M_{S,j}}{DR_j^{D-1}}-2q_D\alpha\gamma\rho_0 R_j. \tag{S19}$$

We also obtain the closed-form and coupled system of ordinary differential equations for the centers $\boldsymbol{x}_{o,j}$ and central wavenumber $\boldsymbol{k}_{o,j}$ of the coherent structure:

$$\partial_t\boldsymbol{x}_{o,j}=\alpha\boldsymbol{k}_{o,j},\quad j=1,2, \tag{S20}$$

$$\partial_t\boldsymbol{k}_{o,j}=-2q_D\gamma\rho_0\boldsymbol{x}_{o,j}-\gamma M_{S,3-j}\frac{\boldsymbol{x}_{o,j}-\boldsymbol{x}_{o,3-j}}{|\boldsymbol{x}_{o,j}-\boldsymbol{x}_{o,3-j}|^D},\quad j=1,2. \tag{S21}$$

A. Mass-radius relation for the hidden soliton

Let us first examine Eq.(S19) for the radius $R_j(t)$ of the j-th soliton component. The energy is of the form $\frac{1}{2}(\partial_t R_j)^2+W_j(R_j)$, with the effective potential

$$W_j(R_j)=\frac{\alpha^2}{2R_j^2}+\sqrt{\frac{2}{\pi}}\frac{\alpha\gamma M_{S,j}}{D(D-2)R_j^{D-2}}+q_D\alpha\gamma\rho_0R_j^2.$$

Equation (S19) has a stable equilibrium $R_j=R_{S,j}$ provided $\partial_{R_j}W_j(R_{S,j})=0$ and $\partial_{R_j}^2W_j(R_{S,j})>0$. For any positive mass $M_{S,j}$, there is a unique stable solution with radius $R_{S,j}(M_{S,j})$ that is the unique solution to the quartic equation

$$M_{S,j}=\sqrt{2\pi}DR_{S,j}^D\bar{\rho}\big((\Lambda/R_{S,j})^4-q_D\rho_0/\bar{\rho}\big). \tag{S22}$$

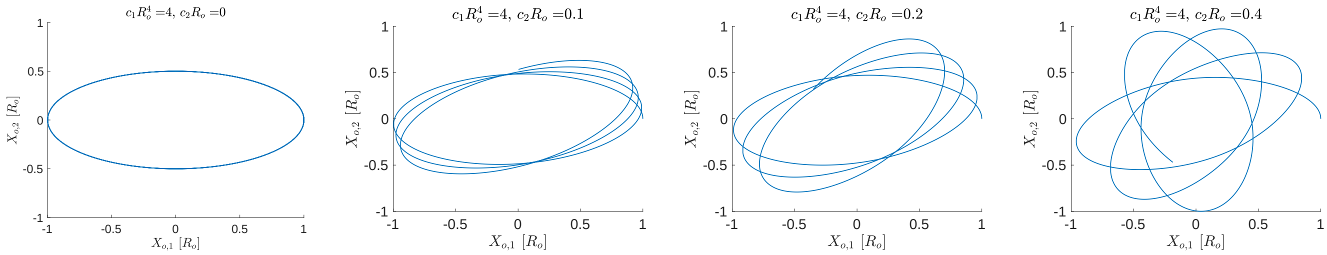

FIG. S1: **Perihelion precession of the 3D binary soliton:** Planar trajectory of the relative motion of the bisoliton $\boldsymbol{X}_o(t)$ for $t \in [0, 10\tau_o]$, $\boldsymbol{X}_o(0) = (R_o, 0, 0)$, $\partial_t \boldsymbol{X}_o(0) \cdot \boldsymbol{X}_o(0) = 0$, $c_o = \partial_t \boldsymbol{X}_o(0) \cdot \boldsymbol{X}_o(0)^\perp = R_o^2/\tau_o$, and for different values of (c_1, c_2).

B. Motion of the center of mass of the binary soliton

1. *Orbital revolution period* $\tau_{\text{c.m.}}$

The soliton barycenter $\boldsymbol{X}_{\text{c.m.}} = (M_{S,1}\boldsymbol{x}_{o,1} + M_{S,2}\boldsymbol{x}_{o,2})/(M_{S,1} + M_{S,2})$, $\boldsymbol{K}_{\text{c.m.}} = (M_{S,1}\boldsymbol{k}_{o,1} + M_{S,2}\boldsymbol{k}_{o,2})/(M_{S,1} + M_{S,2})$ satisfies

$$\partial_t \boldsymbol{X}_{\text{c.m.}} = \partial_{\boldsymbol{K}_{\text{c.m.}}} H_{\text{c.m.}} = \alpha \boldsymbol{K}_{\text{c.m.}}, \tag{S23}$$

$$\partial_t \boldsymbol{K}_{\text{c.m.}} = -\partial_{\boldsymbol{X}_{\text{c.m.}}} H_{\text{c.m.}} = -2q_D\gamma\rho_0 \boldsymbol{X}_{\text{c.m.}}, \tag{S24}$$

with the conserved Hamiltonian $H_{\text{c.m.}} = q_D\gamma\rho_0|\boldsymbol{X}_{\text{c.m.}}|^2 + \frac{\alpha}{2}|\boldsymbol{K}_{\text{c.m.}}|^2$. The coherent structure barycenter then exhibits a periodic ellipsoidal motion in phase-space. The revolution period is $\tau_{\text{c.m.}} = \sqrt{2}\pi/\sqrt{q_D\alpha\gamma\rho_0}$.

2. *The case $D = 3$: Ellipsoidal motion*

For $D = 3$, the motion of $\boldsymbol{X}_{\text{c.m.}}$ lies in a plane (spanned by the initial conditions $\boldsymbol{X}_{\text{c.m.}}(0)$ and $\partial_t \boldsymbol{X}_{\text{c.m.}}(0)$) and follows an ellipse. In the plane of the trajectory, the motion of $\boldsymbol{X}_{\text{c.m.}}$ has the form $\boldsymbol{X}_{\text{c.m.}} = (\mathcal{R}(\theta)\cos\theta, \mathcal{R}(\theta)\sin\theta, 0)$, where

$$\mathcal{R}(\theta) = \frac{c_1^{-1/4}}{\sqrt{w_- \cos^2\theta + w_+ \sin^2\theta}}, \qquad w_\pm = C \pm \sqrt{C^2 - 1}, \qquad \theta(t) = \arctan\Big(w_- \tan(c_o\sqrt{c_1}t)\Big),$$

$c_o = \partial_t \boldsymbol{X}_{\text{c.m.}} \cdot \boldsymbol{X}_{\text{c.m.}}^\perp$ is a constant of motion, $\boldsymbol{X}_{\text{c.m.}}^\perp = (-\mathcal{R}(\theta)\sin\theta, \mathcal{R}(\theta)\cos\theta, 0)$,

$$C = \frac{1}{2\sqrt{c_1}|\boldsymbol{X}_{\text{c.m.}}|^2} + \frac{\sqrt{c_1}|\boldsymbol{X}_{\text{c.m.}}|^2}{2} + \frac{1}{2\sqrt{c_1}c_o^2}\frac{(\boldsymbol{X}_{\text{c.m.}} \cdot \partial_t \boldsymbol{X}_{\text{c.m.}})^2}{|\boldsymbol{X}_{\text{c.m.}}|^2}$$

is a constant of motion, and $c_1 = \frac{4\pi\alpha\gamma\rho_0}{3c_o^2}$. The motion follows an ellipse:

$$w_- X_{\text{c.m.},1}^2 + w_+ X_{\text{c.m.},2}^2 = c_1^{-1/2},$$

where we have assumed that the radius is maximal at time 0 and $\theta(t = 0) = 0$.

C. Relative motion of the binary soliton

The relative motion of the binary soliton is defined from $\boldsymbol{X}_o = \boldsymbol{x}_{o,1} - \boldsymbol{x}_{o,2}$, $\boldsymbol{K}_o = \boldsymbol{k}_{o,1} - \boldsymbol{k}_{o,2}$, which satisfies

$$\partial_t \boldsymbol{X}_o = \partial_{\boldsymbol{K}_o} H_o = \alpha \boldsymbol{K}_o,$$

$$\partial_t \boldsymbol{K}_o = -\partial_{\boldsymbol{X}_o} H_o = -2q_D\gamma\rho_0 \boldsymbol{X}_o - \gamma(M_{S,1} + M_{S,2})\boldsymbol{X}_o/|\boldsymbol{X}_o|^D,$$

with the conserved Hamiltonian $H_o = q_D\gamma\rho_0|\boldsymbol{X}_o|^2 + \gamma(M_{S,1} + M_{S,2})|\boldsymbol{X}_o|^{2-D} + \alpha|\boldsymbol{K}_o|^2/2$.

1. The case $D = 1$: Revolution period $\tau_{\rm bin}$ of the binary soliton

The trajectory has the form of two half ellipses connected through two points that present a small cusp. The relative motion of the binary soliton is then periodic in phase-space with a revolution period

$$\tau_{\rm bin} = \frac{2\sqrt{2}}{\sqrt{\alpha}} \int_0^{\xi(E)} \frac{dx}{\sqrt{E - U(x)}},$$

with $U(x) = \gamma\rho_0 x^2 + \gamma(M_{S,1} + M_{S,2})x$ and $\xi(E) = \big(- \gamma(M_{S,1} + M_{S,2}) + \sqrt{\gamma^2(M_{S,1} + M_{S,2})^2 + 4\gamma\rho_0 E}\big)/(2\gamma\rho_0)$. The integration gives Eq.(10) (main text).

2. The case $D = 3$: Motion of the binary soliton

The motion of $\boldsymbol{X}_o(t)$ lies in a plane. In the plane of the trajectory, the motion of $\boldsymbol{X}_o$ has the form $\boldsymbol{X}_o = (\mathcal{R}(\theta)\cos\theta, \mathcal{R}(\theta)\sin\theta, 0)$, where $u(\theta) = 1/\mathcal{R}(\theta)$ is solution of $\partial_\theta^2 u + u = \frac{c_1}{u^3} + c_2$, and $\theta(t)$ is solution of $\partial_t\theta = \frac{c_o}{\mathcal{R}(\theta)^2}$, where $c_o = \partial_t \boldsymbol{X}_o \cdot \boldsymbol{X}_o^\perp$ is a constant of motion, $\boldsymbol{X}_o^\perp = (-\mathcal{R}(\theta)\sin\theta, \mathcal{R}(\theta)\cos\theta, 0)$,

$$C = \frac{1}{2\sqrt{c_1}|\boldsymbol{X}_o|^2} + \frac{\sqrt{c_1}|\boldsymbol{X}_o|^2}{2} + \frac{1}{2\sqrt{c_1}c_o^2}\frac{(\boldsymbol{X}_o\cdot\partial_t\boldsymbol{X}_o)^2}{|\boldsymbol{X}_o|^2} - \frac{c_2}{\sqrt{c_1}|\boldsymbol{X}_o|}$$

is a constant of motion, and $c_1 = 2q_D\alpha\gamma\rho_0/c_o^2$, $c_2 = \alpha\gamma(M_{\rm S,1} + M_{\rm S,2})/c_o^2$. Note that the function u or $\mathcal{R}$ is periodic in θ, but its period is not 2π (it is 2π if $c_1 = 0$ or $c_2 = 0$). Then the relative motion of the binary soliton is not a closed orbit and it is not periodic, except for some exceptional values of the parameters, see Fig. S1.

3. Computation of the revolution periods of the single soliton and binary soliton in SPE simulations

The evaluation in the simulations of the revolution period of the single soliton in Fig. 3 and of the center of mass of the binary soliton in Fig. 2 requires the computation of the density ρ_0 of the incoherent structure, as well as the mass(es) of the soliton(s) $M_{S,(j)}$. The soliton mass is computed in phase-space from the Husimi function $W(k,x,t)$. In the case of Fig. 3, we obtain $M_S/M = 0.039 \pm 0.002$; in the case of Fig. 2, $M_{S,1}/M = 0.037 \pm 0.002$, $M_{S,2}/M = 0.025 \pm 0.002$. The uncertainties on the masses are determined from the variance of the fluctuations over the relevant time interval. ρ_0 is retrieved by computing the spatial and temporal averages of $\langle|\psi(x,t)|^2\rangle$ over a small spatial window $\Delta x_w \simeq 7.5\Lambda$ and the relevant time interval. In order to account solely for the contribution of the IS component, we have removed the contribution of the soliton mass(es) $M_{S,(j)}$ to the computation of ρ_0. In the case of Fig. 3, we obtain $\rho_0/\bar{\rho} = 4.2 \pm 0.2$; in Fig. 2 $\rho_0/\bar{\rho} = 3.9 \pm 0.2$ (the uncertainties being determined from the variance of the fluctuations). This gives for the single soliton of Fig. 3 $\tau_{\rm c.m.}/\tau = 1.52 \pm 0.04$; and for the binary soliton of Fig. 2 $\tau_{\rm c.m.}/\tau = 1.56 \pm 0.04$, and $\tau_{\rm bin}/\tau = 1.43 \pm 0.04$. These values are in agreement with those observed in the SPE simulations (see the main text: $\tau_{\rm c.m.}^{\rm num}/\tau = 1.52$ for Fig. 3; $\tau_{\rm c.m.}^{\rm num}/\tau = 1.56$, and $\tau_{\rm bin}^{\rm num}/\tau = 1.43$ for Fig. 2).

---

[1] P. Mocz *et al.,* MNRAS **471**, 4559-4570 (2017).
[2] L. Waller *et al.,* Nature Photon. **6**, 474 (2012).
[3] A. Picozzi *et al.,* Physics Reports **542**, 1-132 (2014).
[4] J. Garnier *et al.,* J. Opt. Soc. Amer. B **20**, 1409 (2003).
[5] P. Mocz *et al.,* Phys. Rev. D **97**, 083519 (2018).
[6] C. Uhlemann *et al.,* Phys. Rev. D **90**, 023517 (2014).
[7] B.A. Malomed, Prog. Opt. **43**, 71-193 (2002).